Pd(alkene) adducts is a donor–acceptor π-complex.[10,12] For the Pd(alkane) adducts, the structure might well be the unusual η^2-complex **2**, which was recently predicted by ab initio calculations.[7c]

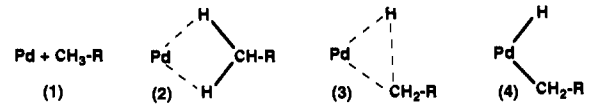

The kinetics measurements are described elsewhere.[12-14] The disappearance of the $4d^{10}$ ($^1S_0$) Pd ground state is monitored by laser-induced fluorescence (LIF).[15] Figure 1 gives several examples of semilogarithmic plots of Pd atom LIF signal vs hydrocarbon number density. The resulting effective bimolecular rate constants k at 300 K and 0.5–0.8 Torr of He are collected in Table I.

Most of the neutral 3d series metal atoms have $3d^{x-2}4s^2$ ground-state configurations.[16] The 4s orbital is larger than 3d;[9] the outer-shell $4s^2$ configuration presents an inert-gas-like appearance to an approaching alkane or alkene, which is itself closed-shell. A substantial potential energy barrier typically prevents close approach of metal atom and hydrocarbon at 300 K. The most reactive atom in the 3d series is Ni,[10,12] whose low-lying $3d^94s^1$ singlet state can form a bound Ni(alkene) complex.[17]

In the 4d series, the 5s and 4d orbitals are more similar in size,[18] which strengthens metal bonding to H and to alkyl. The $4d^{10}$ ground state of Pd is unique among all neutral transition metal atoms. A simple donor–acceptor model of M–alkene bonding predicts that ground-state Pd should fall into a deep attractive well with alkenes, consistent with our observations. The Pd + 1-butene rate constant of 3.5×10^{-10} cm^3 s^{-1} is essentially equal to a hard-spheres collision rate, i.e., the reaction efficiency is 1. Every Pd + 1-butene collision produces an internally hot complex with a sufficiently long lifetime (~50 ns) to be stabilized by He, which implies a deep Pd–butene potential well and no barrier to complex formation.

For Pd + alkane, reaction efficiencies are small, about 5×10^{-4} for C_2H_6, 4×10^{-3} for C_3H_8, and 0.015 for n-C_4H_{10}. We observe no reaction with CH_4 ($k \leq 3 \times 10^{-14}$ cm^3 s^{-1}). The increase in rate constant with He pressure indicates a termolecular reaction in the linear regime of pressure dependence. The lifetime of the internally hot Pd(alkane) complex[13] is probably ~25 ps for C_2H_6, ~200 ps for C_3H_8, and ~0.5 ns for n-C_4H_{10}. The reaction efficiencies suggest that the Pd(alkane) complexes are more weakly bound than the Pd(alkene) complexes. The efficiencies also indicate barriers smaller than 5 kcal mol^{-1} between reactants and the stable Pd(alkane) complex.[12] Exponential decay of Pd signal vs alkane pressure over one decade at 300 K suggests[19] Pd–alkane binding energies of at least 8 kcal mol^{-1} relative to ground-state reactants. These results seem consistent with matrix isolation vibrational spectroscopy[20] of $PdCH_4$.

Recent high-level ab initio calculations suggest the nature of the Pd(alkane) complexes indirectly observed here. Blomberg et al.[7c] examined the reaction path from **1**, M + CH_4, through the transition state **3** to the C–H bond insertion product **4** for all members of the 4d series. For Pd + CH_4, **3** lies 16 kcal mol^{-1} above ground-state reactants **1**; **4** is unstable by 9 kcal mol^{-1} relative to **1**. Pd is unique in that the η^2-complex **2** is a stable minimum below ground-state reactants, with no barrier separating **1** and **2**. The calculated energy of the η^2-complex is only 4 kcal mol^{-1} below reactants, but the geometry was not optimized. The most plausible identity of the inferred Pd(alkane) adducts thus appears to be the η^2-complex.

We plan to extend these kinetics studies to the ground states of ruthenium, rhodium, and platinum to further test the utility of ab initio calculations for such electronically complex systems. We also hope to measure accurate bond energies and to study the novel η^2-complexes spectroscopically in the gas phase.

Acknowledgment. We thank the donors of the Petroleum Research Fund and the National Science Foundation (CHE-9000503) for generous support of this research.

(14) Ritter, D.; Weisshaar, J. C. *J. Phys. Chem.* **1990**, *94*, 4907.
(15) The dye laser excites the $4d^95p$ ($^3D_1$) state at 40 369 cm^{-1}.
(16) Moore, C. E. *National Bureau of Standards Circular No. 467* U.S. Dept. of Commerce: Washington, D.C., 1949; Vols. I–III.
(17) Widmark, P. O.; Roos, B. O.; Siegbahn, P. E. M. *J. Phys. Chem.* **1985**, *89*, 2180.
(18) Carter, E. A.; Goddard, W. A., III *J. Phys. Chem.* **1988**, *92*, 5679.
(19) Ritter, D. Ph.D. Thesis, Department of Chemistry, University of Wisconsin—Madison, Madison, WI, 1990.
(20) Klabunde, K. J.; Jeong, G. H.; Olsen, A. W. In *Selective Hydrocarbon Activation: Principles and Progress*; Bavies, J. A., Watson, P. L., Greenberg, A., Liebman, J. F., Eds.; VCH Publishers: New York, 1990; pp 433–466.

3′-Tetrahydrofuranylglycine as a Novel, Unnatural Amino Acid Surrogate for Asparagine in the Design of Inhibitors of the HIV Protease

Wayne J. Thompson,*,† Arun K. Ghosh,†
M. Katharine Holloway,‡ Hee Yoon Lee,† Peter M. Munson,†
John E. Schwering,† Jenny Wai,† Paul L. Darke,§
Joan Zugay,§ Emilio A. Emini,∥ William A. Schleif,∥
Joel R. Huff,† and Paul S. Anderson†

Departments of Medicinal Chemistry Molecular Biology, Molecular Systems, and Virus and Cell Biology, Merck Research Laboratories West Point, Pennsylvania 19486

Received November 5, 1992

The blockade of the HIV protease has become a major target in the search for an effective therapy for AIDS.[1] While many reports of potent HIV-1 inhibitors have appeared recently, the compound Ro 31-8959 remains the least selective for the HIV-1 and HIV-2 proteases.[2] This property may result in reduced susceptibility to resistance since these represent the genetically most divergent strains of HIV presently known to exist.

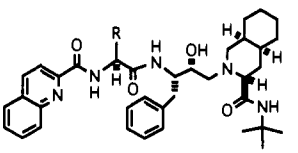

Ro 31-8959, R = CH_2CONH_2
12, R = 3(R)-tetrahydrofuranyl
13, R = 3(S)-tetrahydrofuranyl

Interestingly, no improvement over asparagine at the P_2 subsite has been reported. Computer-assisted modeling starting with the X-ray crystal structure of the L-689,502–HIV-1 protease complex[3] and replacing the L-689,502 inhibitor with Ro 31-8959 suggested that one feasible explanation for this preference might be hydrogen

† Department of Medicinal Chemistry.
‡ Department of Molecular Systems.
§ Department of Molecular Biology.
∥ Department of Virus and Cell Biology.

(1) (a) Huff, J. R. *J. Med. Chem.* **1991**, *34*, 2305–14. (b) Norbeck, D. W.; Kempf, D. J. *Annu. Rep. Med. Chem.* **1991**, *26*, 141–150. (c) Meek, T. D.; Dreyer, G. B. *Ann. N. Y. Acad. Sci.* **1990**, *616*, 41–45.
(2) (a) Roberts, N. A.; Martin, J. A.; Kinchington, D.; Broadhurst, A. V.; Craig, J. C.; Duncan, I. B.; Galpin, S. A.; Handa, B. K.; Kay, J.; Krohn, A.; Lambert, R. W.; Merrett, J. H.; Mills, J. S.; Parkes, K. E. B.; Redshaw, S.; Ritchie, A. J.; Taylor, D. L.; Thomas, G. J.; Machin, P. J. *Science* **1990**, *248*, 358–61. (b) Krohn, A.; Redshaw, S.; Ritchie, J. C.; Graves, B. J.; Hatada, M. H. *J. Med. Chem.* **1991**, *34*, 3340–3342. (c) Craig, J. C.; Duncan, I. B.; Hockley, D.; Greif, C.; Roberts, N. A.; Mills, J. S. *Antiviral Res.* **1991**, *16*, 295–305. (d) Martin, J. A. *Antiviral Res.* **1992**, *17*, 265–278.
(3) Thompson, W. J.; Fitzgerald, P. M. D.; Holloway, M. K.; Emini, E. A.; Darke, P. L.; Tucker, T. J.; Schwering, J. E.; Schleif, W. A.; Quintero, J. C.; Nunberg, J.; Zugay, J. A.; Homnick, C. F.; Springer, J. P.; Huff, J. R. *J. Med. Chem.* **1992**, *35*, 1685–01.

0002-7863/93/1515-801$04.00/0

Scheme I[a]

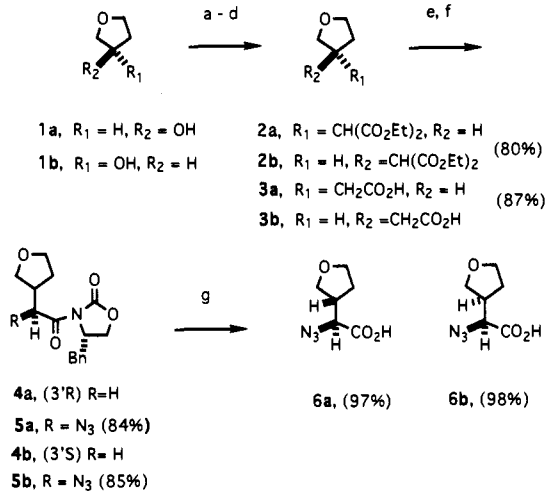

[a] Reagents and conditions: (a) MsCl, Et_3N, 0 °C, CH_2Cl_2; (b) 5 equiv of $(EtO_2C)_2CH_2$, NaH, DMF, 100 °C, 12 h; (c) 1 N NaOH, EtOH, 48 h then HCl; (d) CH_3CN, 0.05 equiv of Cu_2O, 80 °C, 6 h; (e) Me_3COCl, Et_3N, THF, −78 °C then *N*-lithio-(*S*)-(−)-4-benzyloxazolidinone; (f) $KNTMS_2$, THF, −78 °C, 30 min then trisyl azide, −78 °C, 2 min, then AcOH, 30 °C, 30 min; (g) LiOH, THF–H_2O, 45 min.

bonding of the asparagine side chain to the Asp 29 and Asp 30 NH present in the HIV-1 P_2 subsite.[4] Were this model correct, a rigid, cyclically constrained oxygen might be an effective replacement for the primary amide carbonyl oxygen atom. We considered employing the inherent propensity of the tetrahydrofuran (THF) oxygen atom to donate its lone pairs to protons and metal ions as a potential asparagine replacement for the protease enzyme. To test this concept, the unknown (2*S*,3′*R*)- and (2*S*,3′*S*)-tetrahydrofuranylglycines were prepared by chiral synthesis from D- or L-malic acid, respectively, in the following manner.

Enantiomerically pure (*S*)-(+)- and (*R*)-(−)-3-hydroxytetrahydrofurans (**1a** and **1b**) were prepared by acid-catalyzed cyclodehydration of 1,2,4-butanetriol as described by Tandon, van Leuson, and Wynberg.[5] The corresponding mesylates were converted stereospecifically with inversion of configuration into diethyl (*R*)- and (*S*)-3-tetrahydrofuranylmalonates **2a** and **2b** by displacement with the sodium salt of diethyl malonate in DMF at 100 °C.[6] Saponification followed by copper ion promoted decarboxylation[7] afforded the optically pure (*R*)- and (*S*)-3-tetrahydrofuranylacetic acids **3a** and **3b** in excellent yields. The asymmetric azidation methodology of Evans[8] was employed in excellent overall yields for the stereoselective introduction of the α-amino functionality as shown in Scheme I. The hydroxyethylamine isostere **11** was conveniently prepared from the readily available azido diol **7**[9,10] by conversion into the (2*R*,3*S*)-azido epoxide **8**[11,12] followed by reaction with the *tert*-butyl amide of

Scheme II[a]

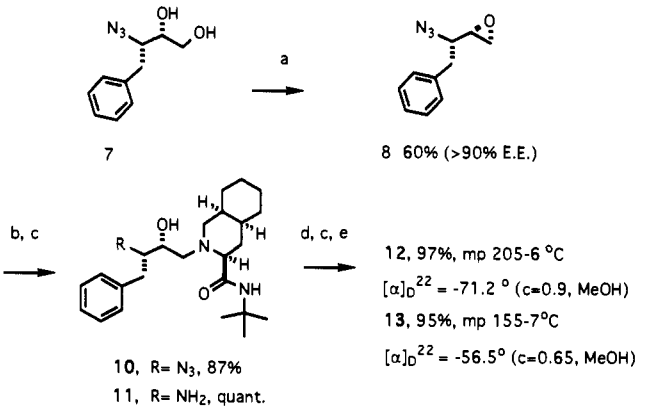

[a] Reagents and conditions: (a) $AcOCMe_2COCl$, 5 h, 25 °C then NaOMe, THF, 3 h, 25 °C; (b) 1.2 equiv of **9**, 80 °C, *i*PrOH, 12 h; (c) H_2 (1 atm), 5% Pd/C, THF, MeOH, AcOH; (d) EDC, HOBt, DMF, *N*-methylmorpholine; (e) quinaldic acid, Ph_2POCl, Et_3N, THF, −10 °C, 1 h, then 12 h, 25 °C.

(3*S*,4a*R*,8a*S*)-decahydroisoquinoline-3-carboxylic acid **9**[13,14] in hot isopropyl alcohol. While the (2*S*,3′*R*)- and (2*S*,3′*S*)-tetrahydrofuranylglycines could be obtained quantitatively from the (2*S*,3′*R*)- and (2*S*,3′*S*)-2-azido-3′-tetrahydrofuranylacetic acids **6a** and **6b** by hydrogenation over a palladium catalyst, we found the α-azido acids to be convenient, chirally stable intermediates for introduction of the 3′-tetrahydrofuranylglycines into the inhibitors (Scheme II).

A comparison of the in vitro potencies of Ro 31-8959 with the tetrahydrofuran-modified inhibitors **12** and **13** was rewarding. The inhibitor derived from (2*S*,3′*R*)-tetrahydrofuranylglycine (3′*R*-Thfg) **12**, IC_{50} = 0.054 ± 0.027 nM (n = 4), was reproducibly 4-fold more potent as a competitive enzyme inhibitor than Ro 31-8959, IC_{50} = 0.23 ± 0.10 nM (n = 3), containing asparagine in the P_2 position. In contrast, the (2*S*,3′*S*)-tetrahydrofuranylglycine (3′*S*-Thfg) **13**, IC_{50} = 5.4 nM (n = 1), was 100-fold less effective than **12**.[15] This strong stereochemical preference supports a hydrogen-bonding phenomenon as an important factor for ligand binding in the P_2 pocket. While the chirality of the HIV-1 protease active site requires a 3′*R*-Thfg, the 3′*S*-Thfg should prove a useful asparagine surrogate for other binding domains in nature.

The activities of the 3-Thfg-derived inhibitors **12** and **13** in the blockade of HIV-1 viral spread in cell culture using MT4 human T-lymphoid cells infected with the IIIb isolate[15] paralleled the inhibitory potencies against the enzyme. In head to head comparison, the 3′*R*-Thfg-derived **12**, CIC_{95} = 8 ± 4 nM (n = 8), was consistently at least 3-fold more potent than the Asn-derived Ro 31-8959, CIC_{95} = 22 ± 7 nM (n = 10), or 3′*S*-Thfg-derived **13**, CIC_{95} > 100 nM.

Finally, the inhibition of HIV-2 protease[16,17] by the 3′-Thfg diastereomer **12** was measured and determined to be 2-fold more potent (IC_{50} = 0.24 nM) than Ro 31-8959 (IC_{50} = 0.5 nM). Further characterization and development of this novel, unnatural amino acid as a protease inhibitor building block are under investigation.[18]

(4) All modeled structures were built using methods described in ref 3. In this model the O–N distances from the Asp side chain oxygen of Ro 31-8959 to the Asp 29 and Asp 30 nitrogen atoms were 2.68 and 3.11 Å. The distances from the 3′*R*-Thfg side chain oxygen atom of inhibitor **15** were 2.81 and 3.21 Å, respectively.

(5) Tandon, V. K.; van Leusen, A. M.; Wynberg, H. *J. Org. Chem.* **1983**, *48*, 2767–2769.

(6) Zaugg, H. E.; Dunnigan, D. A.; Michaels, R. J.; Swett, L. R.; Wang, T. S.; Sommers, A. H.; DeNet, R. W. *J. Org. Chem.* **1960**, *26*, 644–651.

(7) Toussaint, O.; Capdevielle, P.; Maumy, M. *Synthesis* **1986**, 1029–31.

(8) Evans, D. A.; Britton, T. C.; Ellman, J. A.; Dorow, R. L. *J. Am. Chem. Soc.* **1990**, *112*, 4011–30.

(9) Gao, Y.; Hanson, R. M.; Klunder, J. M.; Ko, S. Y.; Masamune, H.; Sharpless, K. B. *J. Am. Chem. Soc.* **1987**, *109*, 5765–80.

(10) Caron, M.; Carlier, P. R.; Sharpless, K. B. *J. Org. Chem.* **1988**, *53*, 5185–7.

(11) For an alternate approach to the *S*-epoxide, see: Rich, D. H.; Sun, C.-Q.; Vara Prasad, J. V. N.; Pathiasseril, A.; Toth, M. V.; Marshall, G. R.; Clare, M.; Mueller, R. A.; Houseman, K. *J. Med. Chem.* **1991**, *34*, 1225–1228.

(12) Russell, A. F.; Greenburg, S.; Moffatt, J. G. *J. Am. Chem. Soc.* **1973**, *95*, 4025–30.

(13) Hayashi, K.; Ozaki, Y.; Nunami, K.-I.; Yoneda, N. *Chem. Pharm. Bull.* **1983**, *31*, 312–4.

(14) (a) Handa, B. K.; Machin, P. J.; Martin, J. A.; Redshaw, S.; Gareth, T. J. *Eur. Pat. Appl.* 0346847A2. (b) Martin, J. A.; Redshaw, S. *Eur. Pat. Appl.* 0432695A2.

(15) For the determination of the inhibitory constants, see ref 3 and references cited therein.

(16) The HIV-2 PR (ROD) was expressed with the same system as the HIV-1 PR which was previously described: Darke, P. L.; Leu, C.-T.; Davis, L. J.; Heimbach, J. C.; Diehl, R. E.; Hill, W. S.; Dixon, R. A. F.; Sigal, I. S. *J. Biol. Chem.* **1989**, *264*, 2307–12.

(17) The HIV-2 PR (ROD) was purified with the same methods as the HIV-1 PR which was previously described: Heimbach, J. C.; Garsky, V. M.; Michelson, S. R.; Dixon, R. A.; Sigal, I. S.; Darke, P. L. Affinity Purification of the HIV-1 Protease. *Biochem. Biophys. Res. Commun.* **1989**, *164*, 955–60.

Supplementary Material Available: Listings of experimental details and spectroscopic characterization for compounds **2-11** and analytical data and stereoview of the optimized bound conformations of Ro 31-8959 and inhibitor **12** superimposed in the inhibited HIV-1 protease active site (8 pages). Ordering information is given on any current masthead page.

(18) Proton NMR and infrared spectra are consistent with assigned structures. Satisfactory (±0.4%) elemental analyses were obtained for new compounds, and all melting points were determined on a Thomas-Hoover capillary melting apparatus and are uncorrected.

Observation of a Small Oligonucleotide Duplex by Electrospray Ionization Mass Spectrometry

K. J. Light-Wahl,† D. L. Springer,‡ B. E. Winger,† C. G. Edmonds,†,‡ D. G. Camp, II,§ B. D. Thrall,‡ and R. D. Smith*,†

Chemical Sciences and Biology and Chemistry Departments, Pacific Northwest Laboratory Richland, Washington 99352 Science Office, Badgley Hall Eastern Oregon State College La Grande, Oregon 97850

Received September 21, 1992

Electrospray ionization (ESI) has been demonstrated to be a "soft" ionization technique, allowing accurate molecular weight determination for biopolymers due to gas-phase multiple charging.[1] Recent results have demonstrated that noncovalent associations can be preserved upon transfer into the gas phase with ESI, providing a new approach to the determination of both structurally-specific[2] and nonspecific[3] noncovalent associations in solution. The mass spectrometric experimental conditions necessary to preserve such noncovalent associations, and the physical constraints upon such, have yet to be elucidated, although it is clear that gentle interface conditions minimizing internal excitation of noncovalent complexes are helpful.[1c,2,3] Base-paired oligonucleotide hybridization constitutes one of the most important and thoroughly studied noncovalent associations of biopolymers. Our initial attempts to observe duplex oligonucleotides resulted in detection of only the monomeric constituents. Since then, we have developed interface conditions that are more gentle and yet still provide sufficient molecular ion desolvation to preserve such associations using new instrumentation with a greatly extended m/z range. In this communication, we report the successful ionization of duplex oligonucleotides and the conditions necessary for detection by negative ion ESI-MS.

Two complementary 20-base single-stranded oligodeoxyribonucleotides were prepared with a DNA synthesizer (Applied Biosystems Model 381A) by phosphoramidite chemistry. The samples were purified by reversed-phase HPLC followed by Centricon 3 (Amicon) ultrafiltration to remove residual salt impurities. Oligonucleotide I contained pyrimidine bases with the sequence 5'-dCCTTCCTCCCTCTCTCCTCC-3' (M_r 5826.9),

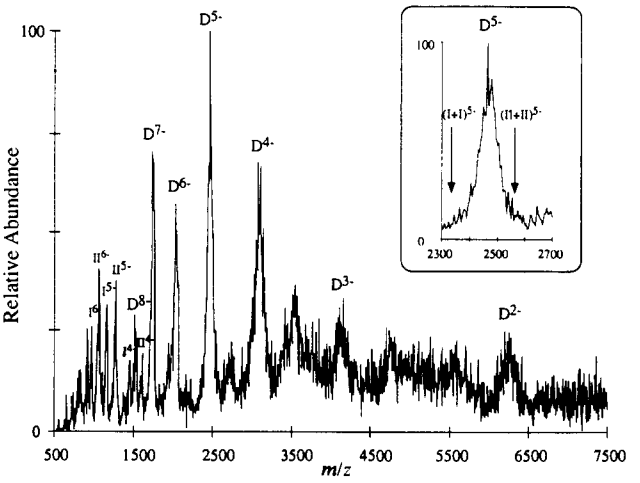

Figure 1. Negative ion ESI mass spectrum of a 20-mer oligodeoxyribonucleotide duplex obtained on the extended m/z range quadrupole mass spectrometer with a mildly heated capillary interface. Capillary–skimmer voltage = 68 V and capillary heating = 23 W (~180 °C at external surface). This spectrum is from the average of five scans consuming approximately 100 pmol. Peaks labeled D are from the duplex ions, and I and II are from the indicated charge states of the complementary single-stranded ions. The insert shows the 5– charge state region of the hybrid duplex ion at m/z ~2446 and the absence of the nonspecific association ions $(I + I)^{5-}$ at m/z 2330 and $(II + II)^{5-}$ at m/z 2563.

and oligonucleotide II was composed of the complementary purine bases with the sequence 5'-dGGAGGAGAGAGGGAG-GAAGG-3' (M_r 6410.3), chosen to avoid ambiguous hybridization of the complementary single strands. Also, their significant differences in M_r allowed potential nonspecific self-association to be resolved under the low-resolution mass spectrometric conditions employed. The purity of the single strands was confirmed by mass spectrometry, and their concentrations were determined by UV spectrophotometry. The single-stranded oligonucleotides (~1×10^{-4} M) were annealed in an aqueous 10 mM NH_4OAc solution by heating to 90–100 °C for 5 min and then slowly cooling to room temperature over 3 h. This solution was chosen to provide sufficient counterions to shield the negatively-charged phosphate groups and facilitate hybridization.

Negative ion ESI mass spectra were obtained using a new extended m/z range (~45 000) quadrupole mass spectrometer developed in our laboratory employing a heated capillary interface.[4] All mass spectra were obtained under conditions intended to minimize heating of molecular ions (i.e., low capillary–skimmer interface voltage, low capillary temperature), but which still provide sufficient excitation to give sufficient desolvation.[5] Figure 1 shows a low-resolution mass spectrum of the hybridized sample in 10 mM NH_4OAc showing multiply charged ions (D^{8-} to D^{2-}) corresponding to the intact duplex (D) dominating at m/z ~2500. It is noteworthy that, while both single-stranded constituents (I and II) are observed at low m/z, the duplex form is predominant at higher m/z. The insert in Figure 1 shows an expansion of the m/z region of the 5^- charge state of the double-stranded duplex ion (D^{5-}) at m/z 2446 corresponding to the specific hybridization of the complementary single-stranded species (I + II). Homodimeric association of each strand during the electrospray process would be expected to produce additional 5– ions at m/z 2330 (I + I) and m/z 2563 (II + II) which are not observed, indicating that a more specific association in solution was involved in producing the duplex ions. As expected, the intact duplex was not observed when distilled deionized water was substituted as the

* Author to whom correspondence should be addressed.
† Chemical Sciences Department, Pacific Northwest Laboratory.
‡ Biology and Chemistry Department, Pacific Northwest Laboratory.
§ Eastern Oregon State College.

(1) (a) Fenn, J. B.; Mann, M.; Meng, C. K.; Wong, S. F.; Whitehouse, C. M. *Science* **1989**, *246*, 64. (b) Fenn, J. B.; Mann, M.; Meng, C. K.; Wong, S. F. *Mass Spectrom. Rev.* **1990**, *9*, 37. (c) Smith, R. D.; Loo, J. A.; Ogorzalek Loo, R. R.; Busman, M.; Udseth, H. R. *Mass Spectrom. Rev.* **1991**, *10*, 359. (d) Smith, R. D.; Loo, J. A.; Edmonds, C. G.; Barinaga, C. J.; Udseth, H. R. *Anal. Chem.* **1990**, *62*, 882.

(2) (a) Ganem, B.; Li, Y.-T.; Henion, J. *J. Am. Chem. Soc.* **1991**, *113*, 6294. (b) Ganem, B.; Li, Y.-T.; Henion, J. *J. Am. Chem. Soc.* **1991**, *113*, 7818. (c) Katta, V.; Chait, B. T. *J. Am. Chem. Soc.* **1991**, *113*, 8534. (d) Baca, M.; Kent, S. B. H. *J. Am. Chem. Soc.* **1992**, *114*, 3992. (e) Ganguly, A. K.; Pramanki, B. N.; Tsarbopoulos, A.; Covey, T. R.; Huang, E.; Fuhrman, S. A. *J. Am. Chem. Soc.* **1992**, *114*, 6559.

(3) Smith, R. D.; Light-Wahl, K. J.; Winger, B. E.; Loo, J. A. *Org. Mass Spectrom.* **1992**, *27*, 811.

(4) (a) Chowdhury, S. K.; Katta, V.; Chait, B. T. *Rapid Commun. Mass Spectrom.* **1990**, *4*, 81. (b) Rockwood, A. L.; Busman, M.; Udseth, H. R.; Smith, R. D. *Rapid Commun. Mass Spectrom.* **1991**, *5*, 582.

(5) Electrospray conditions utilized a 0.4 μL/min sample flow, a methanol sheath (3.0 μL/min), a coaxial flow of SF_6 (~100 mL/min) which serves to suppress electrical discharges during negative ion production, and a countercurrent flow of heated N_2 for desolvation. An aqueous sheath flow gave similar mass spectra but weaker ion signals.

0002-7863/93/1515-803$04.00/0